

Lawrence Berkeley National Laboratory

Recent Work

Title

THE JOSEPHSON JUNCTION AS A DETECTOR OF MICROWAVE AND FAR INFRARED RADIATION

Permalink

<https://escholarship.org/uc/item/3949b098>

Author

Richards, P.L.

Publication Date

1969-06-01

To be published as a Chapter in book
Physics of III-V Compounds, Vol. 6
(Academic Press, N. Y.)

UCRL-19035
Preprint

yz

RECEIVED
LAWRENCE
RADIATION LABORATORY

THE JOSEPHSON JUNCTION AS A DETECTOR OF
MICROWAVE AND FAR INFRARED RADIATION

DEC 16 1969

LIBRARY AND
DOCUMENTS SECTION

P. L. Richards

June 1969

AEC Contract No. W-7405-eng-48

TWO-WEEK LOAN COPY

*This is a Library Circulating Copy
which may be borrowed for two weeks.
For a personal retention copy, call
Tech. Info. Division, Ext. 5545*

LAWRENCE RADIATION LABORATORY
UNIVERSITY of CALIFORNIA BERKELEY

UCRL-19035

DISCLAIMER

This document was prepared as an account of work sponsored by the United States Government. While this document is believed to contain correct information, neither the United States Government nor any agency thereof, nor the Regents of the University of California, nor any of their employees, makes any warranty, express or implied, or assumes any legal responsibility for the accuracy, completeness, or usefulness of any information, apparatus, product, or process disclosed, or represents that its use would not infringe privately owned rights. Reference herein to any specific commercial product, process, or service by its trade name, trademark, manufacturer, or otherwise, does not necessarily constitute or imply its endorsement, recommendation, or favoring by the United States Government or any agency thereof, or the Regents of the University of California. The views and opinions of authors expressed herein do not necessarily state or reflect those of the United States Government or any agency thereof or the Regents of the University of California.

THE JOSEPHSON JUNCTION AS A DETECTOR OF MICROWAVE
AND FAR INFRARED RADIATION

P. L. Richards

Department of Physics and Inorganic Materials Research Division, and
Lawrence Radiation Laboratory, University of California, Berkeley, Ca. 94720

I. INTRODUCTION

The macroscopic quantum phenomena associated with the superconducting state provide a unique bridge between the microscopic quantum "world" and the macroscopic world of everyday experience. They are, therefore, much studied because of their intrinsic interest. For the purposes of this volume, however, we will consider only those aspects of the phenomena which involve the interaction of electromagnetic waves with weak links between superconductors.

Most of those effects discussed here were predicted theoretically by B. D. Josephson¹ from the quantum theory of tunneling through a thin oxide barrier between two plane superconducting films. The tunneling current through such a junction has been studied extensively. It can be divided into two parts: single particle tunneling and Josephson tunneling. The first to be discovered was the tunneling of individual electrons or quasiparticles, which usually dominates the dc current when voltages comparable to the energy gap are applied. This effect has been widely used for the study of the energy gap in the density of states for excitations from the superconducting ground state.² Josephson showed that correlated "superconducting" pairs of electrons will also tunnel and should allow current flow with no associated voltage drop. This Josephson current is extremely sensitive to electromagnetic fields in a way which permits the construction of a variety of sensitive detectors of radiation at frequencies up to the far-infrared. Regenerative and heterodyne, as well as video modes of detection, are possible.

The fundamental limit on the frequency response of all such devices is set by the gap energy of the superconductor employed. Radiation with

quantum energies large compared with this gap excites particles from the ground state of the superconductor and thus interacts in a way more characteristic of a normal than a superconducting metal. The energy gap 2Δ is typically $3.5 - 4 kT_c$ where T_c is the critical temperature of the superconductor. Calculations by Riedel³ and by Werthamer⁴ summarized in Fig. 1 show that the kernel which determines the frequency dependence of the Josephson current amplitude peaks at 2Δ and has a reasonable amplitude at frequencies at least as high as 4Δ . Josephson effect detectors made from Nb with $T_c \sim 8^\circ\text{K}$ should thus operate at frequencies above 50 cm^{-1} , while compound superconductors such as Nb_3S_n with $T_c \sim 17^\circ\text{K}$ should in principle be useful well above 100 cm^{-1} .

II. THE ALTERNATING CURRENT JOSEPHSON EFFECT

An elementary discussion of the ac Josephson effect intended for the uninitiated is presented in this section. Readers who are familiar with the effect may wish to skip to Section III. Any discussion of the Josephson effect must be quantum mechanical since no valid classical description is known. The wave function, or order parameter, for the superconducting state can be written in the simple form $\psi = \psi_0 e^{i\theta}$, where the phase factor is a function of both position and time. Josephson's calculations showed that his lossless pair tunneling current depends on $\Delta\theta$ the phase difference between the wave functions for the superconductors on the two sides of the tunnel junction¹

$$I = I_0 \sin \Delta\theta. \quad (1)$$

Here I_0 is the maximum zero-voltage current which can be carried by the

junction.

We will consider the effect of the finite potential drop V across an oxide barrier which occurs when I_0 is exceeded. The quantum theory of tunneling¹ then predicts a time dependence of the phase difference

$$\frac{\hbar d(\Delta\theta)}{dt} = 2eV. \quad (2)$$

This result for superconductors is analogous to that obtained from the elementary quantum mechanics of a single particle system. If we assume a wave function of the above form and use Schrodinger's equation for a single particle, $-\hbar^2 \nabla^2 \psi = \mathcal{H}\psi$, the time dependence of the phase difference $\Delta\theta$ between two states is $\hbar d(\Delta\theta)/dt = \Delta E$. In Josephson's result (2) for the superconducting tunnel junction, the chemical potential difference or change in system energy $2eV$ when a superconducting pair moves from one side of the barrier to the other plays the role of ΔE , the energy difference between the two single particle states.

If the voltage V_0 is constant in time, Eq. (2) can be integrated to give $\Delta\theta = 2eV_0 t/\hbar + \theta_0$. Equation (1) then predicts an alternating current flow across the barrier at the frequency $\omega_0 = 2eV_0/\hbar$. The Josephson junction is thus a quantum mechanical oscillator. Its frequency can be high since $\omega_0/2\pi = 484 \text{ GHz/mV}$. The existence of this Josephson alternating current has been verified by observing^{5,6} microwave radiation emitted at the frequency ω_0 . The ac Josephson currents were first detected, however, by an easier experiment.⁷ An alternating voltage $V_1 \cos\omega_1 t$ at a microwave frequency ω_1 was induced across the barrier in addition to the steady voltage V_0 . Equation (2) then yields

$$\Delta\theta = (2eV_0 t/\hbar) + (2eV_1 \sin\omega_1 t/\hbar\omega_1) + \theta_0,$$

so from Eq. (1)

$$I(t) = I_0 \sin [(2eV_0 t/\hbar) + (2eV_1/\hbar\omega_1) \sin\omega_1 t + \theta_0]. \quad (3)$$

This equation shows that the frequency of $I(t)$ is modulated by the microwave frequency ω_1 . It is usual to expand such expressions using the relations

$$\cos(X \sin\alpha) = \sum_{n=-\infty}^{\infty} J_n(X) \cos(n\alpha)$$

and

$$\sin(X \sin\alpha) = \sum_{n=-\infty}^{\infty} J_n(X) \sin(n\alpha)$$

where $J_n(X) = (-1)^n J_{-n}(X)$ is Bessel's function of order n . Choosing the value $\theta_0 = \pi/2$ which corresponds to a maximum zero-voltage current ($V_0 = \omega_0 = 0$) and using standard trigonometric identities, we obtain

$$I = I_0 \sum_{n=-\infty}^{\infty} J_n\left(\frac{2eV_1}{\hbar\omega_1}\right) \cos(\omega_0 + n\omega_1)t. \quad (4)$$

The junction is thus a nonlinear device in which the Josephson currents beat with the induced ac signal. In order to operate it as a detector we measure the zero frequency beats which occur when $\omega_0 + n\omega_1 = 0$. Then

$$I_{dc} = I_0 (-1)^n J_n\left(\frac{2eV_1}{\hbar\omega_1}\right). \quad (5)$$

A lossless contribution to the dc current appears whenever the voltage is adjusted so that the ac Josephson frequency $\omega_0 = 2eV_0/\hbar$ equals harmonics of the microwave frequency ω_1 . The amplitude of this dc beat

current is given by Bessel's functions $J_n(2eV_1/\hbar\omega_1)$, where n is the order of the harmonic.

The observation of constant voltage steps on the I-V characteristic of a Josephson junction placed in a microwave field thus verifies the existence of the ac Josephson currents. Examples of such I-V characteristics are shown in Fig. 2. This experiment has considerable practical importance. Careful measurements of the applied microwave frequency and the voltage at which the steps occur have recently yielded the best numerical value for the ratio of fundamental constants e/h .⁸

III. HETERODYNE DETECTOR WITH JOSEPHSON FREQUENCY AS LOCAL OSCILLATOR

The constant-voltage steps shown in Fig. 2 can be interpreted as a zero frequency beat between the n th harmonic of the induced rf radiation and the ac Josephson current. A type of heterodyne detector is thus obtained if the height of one of the steps is monitored. For small values of the signal voltage

$$I_{dc} = \frac{I_0}{n!} \left(\frac{eV_1}{\hbar\omega_1} \right)^n \quad (6)$$

so that measuring the $n=1$ step gives a linear detector, the $n=2$ step a square law detector, etc.

Most applications of a Josephson junction as a radiation detector require the measurement of the amplitude of a constant-voltage step. This is usually done by biasing the junction with a constant current in a region of high differential resistance (small slope) associated with the step as is shown in Fig. 3a. As the height of the step changes due to a modulated rf signal, the junction voltage varies at the modulation

frequency. A conventional lock-in amplifier is then used to extract the signal. In this method the output signal is proportional to the differential resistance and thus, approximately, to the step height.

The attractively simple heterodyne detector described above has several defects related to this method of measuring step height. It cannot be used for small signals since a large radiation-induced step is needed for high sensitivity. Good frequency selectivity is also difficult to obtain in practice from a Josephson junction operated in this mode. This measurement of the height of a given step is also sensitive to changes in the I-V curve due to neighboring steps so that a range of frequencies is detected.

An alternative bias scheme which has not yet been used may reduce some of these limitations. A constant voltage bias can be achieved by passing a constant current through a very small resistance (perhaps $10^{-6}\Omega$) in parallel with the junction. A transformer coupled superconducting galvanometer⁹ in series with the junction can then be used to measure the current. In order to measure the height of a step, the voltage should be modulated with small amplitude about the step voltage and the resulting ac current measured as shown in Fig. 3b. A detector operated in this way is sensitive to the rate of change of I_{dc} with V_1 , V_1^2 , ... etc., without the requirement of a large step to produce a region of high differential resistance. It should thus be sensitive to small signals and also relatively insensitive to changes in the I-V curve due to steps outside the range of the bias voltage modulation.

Several defects of the heterodyne detector described here remain even with constant voltage bias. In a conventional heterodyne detector

the small signal responsivity can be raised by increasing the local oscillator voltage. In our case, the ac Josephson current is limited by junction parameters to unfavorably small values. In addition, because of the extreme non-linearity of its response, a Josephson junction biased to detect the n th step for a signal frequency ω_1 has comparable sensitivity to signals at all subharmonics of ω_1 . If other types of weak-link structures are used,^{10,11} sensitivity can also occur at harmonics of ω_1 .

IV. BROAD BAND VIDEO DETECTOR

In the limit of small rf signal, only the step at zero voltage (the zero voltage current) has finite amplitude. Since with conventional constant-current bias, the sensitivity with which a change in step height is measured increases with step height, a practical detector for small signals can be made by biasing the junction so as to monitor the zero voltage current. Since $n=0$ for this $V_0=0$ step, the condition for direct current, $2eV_0/\hbar = \pm n\omega_1$ is automatically satisfied for all ω_1 . This broad band detector has a square-law response for small signals. From Eq. (5)

$$\frac{dI_{dc}}{dV_1^2} = \frac{-I_0}{4} \left(\frac{2e}{\hbar\omega_1} \right)^2. \quad (7)$$

The spectral response of point contact detectors of this type, which were first studied by Grimes, Richards, and Shapiro,¹² is strongly conditioned by several factors which tend to mask the Riedel singularity shown in Fig. 1. These include the ω_1^{-2} dependence of the square-law response from Eq. (7) as well as the effects of junction capacitance and resonances in the surrounding structures. Figs. 4 and 5 show extremes

of spectral response resulting from various methods of constructing and mounting point contact Josephson junctions. Because the observed response peaks are uncorrelated with the energy gap frequency, it seems safe to say that these results are dominated by cavity resonances rather than the Riedel singularity.

V. REGENERATIVE DETECTOR

As we have seen, the presence of cavity resonances coupled to a Josephson junction strongly affects its response as a broad band detector. The theory of the Josephson effect has been extended to include such effects.¹² This theory is rather too involved to present in detail, but a simplified summary can be given. The voltage $V(t)$ across the junction is obtained by treating the resonant cavity as a driven harmonic oscillator with frequency ω_c , and damping constant γ .

$$\left(\frac{d^2}{dt^2} + \gamma \frac{d}{dt} + \omega_c^2 \right) \frac{2eV(t)}{\hbar} = F(t). \quad (8)$$

The cavity is driven by both the Josephson current $I(t)$ in the junction and the applied rf voltage $V_1 \cos(\omega_1 t + \phi)$.

$$F(t) = A \frac{dI}{dt} + B V_1 \cos(\omega_1 t + \phi) \quad (9)$$

where the Josephson current, as usual, is

$$I(t) = I_0 \sin \left[\left(\frac{2eV_0 t}{\hbar} \right) + \frac{2e}{\hbar} \int^t V(t') dt' + \pi/2 \right]. \quad (10)$$

Here A and B are coefficients which measure the coupling of the Josephson current to the cavity response and the coupling of the applied radiation to the cavity respectively. This non-linear differential equation was solved for $V(t)$ and the resulting I_{dc} computed by Werthamer and Shapiro¹²

for the case $V_1=0$. They found that when the dc voltage is adjusted to a cavity mode, $2eV_0 \approx \hbar\omega_c$, the Josephson current can excite the cavity mode with sufficient amplitude that steps are induced on the I-V curve similar to these produced by an external monochromatic rf voltage. Such "cavity mode steps" were first reported by Fiske¹⁴ in self-resonant evaporated film junctions and are also¹⁵ seen for point contact junctions in a resonant cavity.

These self-induced cavity mode steps have been used by Richards and Sterling¹⁶ to construct a regenerative detector. They used the constant current technique illustrated in Fig. 3a to measure the response of the cavity mode step to broadband rf radiation. In order to interpret their results they extended the theory of Werthamer and Shapiro to the case of applied rf in the vicinity of the cavity mode frequency, $\omega_1 = \omega_0 \approx \omega_c$ and computed the step height, I_{dc} , as a function of V_1 and ω_1 . The results of this calculation can best be summarized by reference to the simplified regenerative receiver circuit shown in Fig. 6. If the feedback loop is broken, a signal from the antenna passes through a resonant band-pass filter characterized by ω_c and quality factor $Q_c = \frac{\omega_c}{\gamma}$ and then through an amplifier to a detector. This is the case of broadband response when the junction is biased so as to measure the zero voltage current. The frequency response is multiplied by a Lorentzian resonance factor due to the cavity to which the junction is coupled. The broadband response of Section IV can thus be used to measure Q_c . If, on the other hand, the junction is biased so that $\omega_0 \approx \omega_c$, the Josephson radiation excites the cavity mode and is fed back to the junction in such a way as to create a step, the feedback loop in

Fig. 6 is then closed with positive phase. As the loop gain G_L is increased the response $Q_R \approx (1-G_L)^{-1}$ of the receiver increases. When $G_L=1$ the receiver will oscillate around the loop. The calculated normalized spectral response of the resonant junction is shown in Fig. 7. As the feedback parameter Γ increases, the detector response sharpens from the Lorentzian cavity mode at $\Gamma=1$ to oscillation for $\Gamma \geq 2.9$.

The operation of a regenerative detector of this type is in good qualitative agreement with the theory outlined here.¹⁶ Fig. 8 shows a plot of the I-V curve, the differential resistance, and the sensitivity to a modulated blackbody source of a resonant point contact junction. The broadband response of Section IV dominates the sensitivity plot, but a small peak due to the regenerative response is also seen. The spectral response of a regenerative detector measured using a blackbody source and far infrared Fourier transform spectroscopy is shown in Fig. 9. Although the peak is not resolved, the effect of feedback narrowing is clearly seen. The response Q_R is estimated in this case to be at least 100 times greater than the cavity $Q_c \approx 10$ measured from its influence on the broadband response discussed in Section IV. It is a property of the Fourier transform method that non-square law response of the detector generates spurious harmonics in the computed spectra. The absence of harmonic peaks in spectra such as Fig. 9 confirms the predicted square-law response of the regenerative detector. A linear response is also expected, but only within a very narrow bandwidth around ω_c determined by the post-detection time constant. This linear response is negligible in experiments with broadband sources, but may be important under other conditions. It is essentially heterodyne detection with the cavity mode as local oscillator.

The regenerative detector has several favorable features. It is a

sensitive narrow-band device whose frequency and Q_R can be selected over a wide range by proper cavity design. If the cavity has several resonances coupled strongly to the junction, narrow band detection can be obtained at each frequency simply by adjusting V_0 to the region of high differential resistance caused by the appropriate cavity mode step.

VI. MIXER

Many of the undesirable features of the type of Heterodyne receiver described in Section III can be avoided by using the Josephson junction as a mixer in connection with an external local oscillator. The mixing properties of point contact Josephson junctions have been studied by Grimes and Shapiro¹⁷ using the theory of Section II. If we induce two alternating voltages across the barrier,

$$V = V_0 + V_1 \cos(\omega_1 t + \theta_1) + V_2 \cos(\omega_2 t + \theta_2), \quad (11)$$

then Eq. (4) becomes

$$I = I_0 \sum_{n,m=-\infty}^{\infty} J_n \left(\frac{2eV_1}{\hbar\omega_1} \right) J_m \left(\frac{2eV_2}{\hbar\omega_2} \right) \sin \left[\omega_0 t + \theta_0 + n(\omega_1 t + \theta_1) + m(\omega_2 t + \theta_2) \right]. \quad (12)$$

Eq. (12) is the general expression for the Josephson currents at all frequencies and voltages in the presence of two applied rf voltages.

It predicts the appearance of dc (current) steps whenever

$\omega_0 + n\omega_1 + m\omega_2 = 0$, where n and m are integers with all positive and negative values. These include the familiar steps expected for each frequency acting separately, as well as steps spaced by multiples of the difference frequency $\omega_1 - \omega_2$ from the steps associated with each

frequency acting alone. These extra steps which are illustrated in Fig. 10 are evidence for mixing in a Josephson junction. As is the case of θ_0 in Eq. (3), Eq. (12) contains a phase factor which is fixed by the amount of zero-voltage current driven through the junction by the external source. For simplicity we will again limit our consideration to detectors biased so as to measure the maximum zero-voltage current on any step so that $\theta_0 + n \theta_1 + m \theta_2 = \pi/2$.

Grimes and Shapiro considered several cases of mixing of millimeter waves in a Josephson junction. The cases of primary interest to us are those in which a weak signal is applied at the frequency ω_2 which is nearly equal to the fundamental (or a harmonic of) the frequency ω_1 of a strong local oscillator. In this case the two signals are equivalent to one applied signal which is slightly modulated at the low frequency $\omega_1 - \omega_2$. The theory of the heterodyne detector is thus closely related to that of the video detector of Section IV. The sensitivity of both detectors is proportional to the differential resistance of the static I-V curve of the junction. This behavior is in sharp contrast to the classical mixer response which is proportional to the curvature of the I-V curve, i.e., to the square of the differential resistance. In the present case, we have a strong signal which is only slightly modulated. This strong signal creates current steps on the I-V

characteristic and there is a peak in the response of the heterodyne detector in the high differential resistance region associated with each step. We may contrast this with the conditions found in Section IV where there was only one (zero voltage) step and thus only one region of sensitivity. The bandwidth of this heterodyne detector is, as usual, determined by the intermediate frequency (if) system employed. Grimes and Shapiro have verified this analysis using mm microwave sources and an if bandpass in the range from ~ 1 to 150 MHz. Heterodyne detectors based on these principles could be operated at higher frequencies by using a far infrared laser source for the local oscillator.

In a related set of experiments, S. Shapiro¹⁸ has studied the mixing of an applied rf signal with the currents in a resonant junction which flow at the cavity mode frequency. Steps at the sum and difference between the cavity mode step and an induced rf step are predicted in the Werthamer-Shapiro theory and are seen experimentally. This effect can be interpreted as a parametric process in which a step is created at the difference voltage by rf energy at the signal frequency which results from the applied rf pump and the cavity mode idler frequency.

VII. THE IMPEDANCE PROBLEM

In order for a Josephson junction to function efficiently as a detector of electromagnetic radiation, the power incident P_o in a free space wave or waveguide of impedance Z_o must be matched to the junction so as to obtain the largest possible V_1^2 . If the junction impedance is Z_1 and a perfect impedance transformer is used then

$$V_1^2 = Z_1 P_o \quad (13)$$

Even in this case a large junction impedance is desirable. If the impedance match is less than perfect, Eq. (13) must be multiplied by a power transmission factor. In the worst case of no matching

$$V_1^2 = 4 \frac{Z_1^2 Z_0}{(Z_1 + Z_0)^2} P_0. \quad (14)$$

Clearly, the matching problem is more difficult for small values of Z_1 . The lack of a suitable high impedance junction is the major problem limiting the usefulness of Josephson effect detectors. Evaporated film (pure Josephson) junctions have a necessarily large capacitance. The various weak link junctions such as Dayem bridges,¹⁰ Proximity effect bridges,¹⁹ or SNS sandwiches¹¹ also have very low impedance. Most of the current work on detectors has used point contact junctions. Such junctions are too delicate to be suitable for practical detectors. For example, only rarely will the properties required for good detection sensitivity survive a temperature cycle between 4K and 300K. Comparison of the shape of the I-V curves of good point contact detectors with theory²⁰ indicates that Z_1 is largely resistive and of the order of 1Ω . This resistance, which can be imagined to arise from metallic short circuits which carry currents larger than their superconducting critical current, can have large effects on the Q of a cavity coupled to the point contacts. Of course, any frequency dependent (reactive) component in the impedance of the junction will complicate the spectral response of broadband detectors. It is often found that the spectral response falls off more rapidly with frequency than is expected from Fig. 1 and Eq. (7). It thus seems possible that capacitance in point contact junctions

becomes important at the highest frequencies.

Point contacts can be made from most any superconductor, but Nb is perhaps the most commonly used. The usual procedure is to form a point of radius $\approx 25 \mu$ on one Nb wire and a flat on another and to set them aside for several days to oxidize. The wires are then mounted in a stable constant-force arrangement such as that shown in Fig. 12 and the contact gently made at He temperature. An extensive review of the properties of superconducting point contacts is in press.²²

Several techniques have been used to couple point contact junctions to radiation in light pipes or resonant cavities. All of these structures are more or less resonant. The simplest procedure is to mount the points transversely across a waveguide or light pipe (oversized waveguide) so that the E-field induces currents in the junction. The guide can be terminated non-resonantly, or with an adjustable matching plunger. Several typical far-infrared cavities are shown in Fig. 11. The most useful resonant geometries appear to be the co-axial resonator with the junction located in the center conductor, and the Fabry-Perot resonator.

T. D. Clark²¹ has studied the properties of an array of point contacts constructed from a layer of superconducting balls in a planar hexagonal lattice. Despite difficulties with uniformity of the contacts between the balls, effects have been seen which correspond to the broadband detection of Section IV and the regenerative detection of Section V. These results seem to indicate that the contacts are radiatively coupled so that under favorable circumstances the voltage drop can be the same for each of a line of contacts in series. An alternative coupling philosophy is to mount the junction in a conducting loop which is threaded by the rf magnetic field. This method has been

less used because of the difficulty of measuring the junction current. In spite of this difficulty the method has considerable promise and will be discussed in the next section.

VIII. MAGNETIC COUPLING

One potentially useful detector geometry which has not been widely exploited is that of a junction located in a conducting loop. Such a loop can be inductively coupled to the rf magnetic field in a resonant cavity. The junction must be the largest impedance in the loop in order to induce a large V_1 . Most previously-used co-axial cavities do not satisfy this requirement as the center conductor (which includes the point contact) is insulated from the cavity to permit mechanical adjustment and dc bias measurements. The capacitive reactance of such insulating sleeves is often large compared with the junction impedance. Some improvement may thus be expected if low impedance isolation capacitors (such as evaporated films) are used.

The chief advantage of magnetic coupling is, however, lost if such isolation capacitors are required. By the use of a continuous superconducting loop, it is possible to couple efficiently to any of the rugged, reliable, very low impedance weak link junctions such as the Dayem bridge¹⁰ or the proximity effect bridge.¹⁹ The practical advantages in abandoning the fragile point contact junction seem very important. The problems of bias and information retrieval from superconducting loops with weak links have been studied extensively by workers interested in constructing static magnetometers.²³⁻²⁵ If the loop contains two

junctions, constant current bias similar to that described in Sec. III can be used. Magnetometer development, however, has favored a loop with a single junction.^{24,25} Nuclear magnetic resonance techniques are then used to bias the ring and to measure its ac-impedance in the MHz frequency range. The theory of the Josephson junction developed in Sec. II can be used to qualitatively understand the behavior of any weak link. The theory is not strictly valid since Eq. (1) should be replaced by a more general periodic function with high harmonic content,¹⁰ but it is sufficient for our purposes. If the link is connected in a superconducting loop, the static voltage V_0 , and the Josephson frequency $\omega_0 = 0$. In order to understand the effects of a static flux Φ (with vector potential A) threading a multiply connected superconductor, the theory of Sec. II must be extended to include the effects of quantization of the canonical momentum $2mv + 2eA/c$ around the loop. If this is done, Eq. (4) contains a factor $\cos(2\pi\Phi/\Phi_0)$, that is, the critical current of the junction is a periodic function of Φ with a maximum whenever Φ is a multiple of the flux quantum $\Phi_0 = hc/2e$. From Eq. (4) we can compute the current I_{ω_1} at the frequency of an induced voltage $V_1 = \omega_1\Phi_1/c$ where Φ_1 is the ac flux from the measuring circuit.

$$I_{\omega_1} = I_0 J_1\left(\frac{2\pi\Phi_1}{\Phi_0}\right) \cos(\omega_1 t) \cos\left(\frac{2\pi\Phi}{\Phi_0}\right). \quad (15)$$

This magnetometer equation shows that the ac impedance is a periodic function of the static flux Φ with period Φ_0 . We can use Eq. (15) to describe a magnetically coupled electromagnetic wave detector if we let the static flux include the flux at the signal frequency

$\Phi \rightarrow \Phi + \Phi_2 \sin \omega_2 t$ and use the Bessel's function expansion described in

Sec. II. Alternatively we can use the mixer equation (11) with $\omega_0 = 0$ to compute the current at the measuring frequency $I(\omega_1)$ due to voltages $V_1 = \omega_1 \Phi_1 / c$ induced by the measuring circuit and $V_2 = \omega_2 \Phi_2$ induced by the signal.

$$I_{\omega_1} = I_1 J_1\left(\frac{2\pi\Phi_1}{\Phi_0}\right) J_0\left(\frac{2\pi\Phi_2}{\Phi_0}\right) \cos(\omega_1 t) \cos\left(\frac{2\pi\Phi}{\Phi_0}\right). \quad (16)$$

The effect of a static flux Φ has been included for completeness. Notice that Eq. (16) describes a broadband detector since ω_2 does not appear. Various types of narrow band detectors could, of course, be constructed by measuring the current at some frequency $n\omega_1 \pm m\omega_2$.

IX. CONCLUSIONS

Superconducting Josephson effect detectors for the millimeter wave and far infrared frequency regions are in an early stage of development. The feasibility of several types of detectors has been proved using point contact junctions which have poor mechanical properties. These experiments have generally been limited by noise from the junction, notably from fluctuations in the trapped magnetic flux. The most important outstanding problem is obtaining good coupling between the junction and the rf fields. A good coupling scheme would permit the use of the rugged quiet Dayem bridge or other low impedance junction.

The importance of improving the coupling can be illustrated by considering the dc magnetometers currently constructed²⁵ from a superconducting loop of mm dimensions containing a single Dayem bridge. A field sensitivity of $\sim 10^{-10}$ gauss is obtained in a one Hz bandwidth and the limiting noise comes from the external circuit. If the magnetic field from an electromagnetic wave were efficiently coupled to such a

magnetometer, a millimeter wave detector with a power sensitivity of $\sim 10^{-20}$ W/ $\sqrt{\text{Hz}}$ would result. This number is very much better than the current results of $\sim 10^{-13}$ W/ $\sqrt{\text{Hz}}$ for the analogous broadband point contact detector of Sec. IV and the $\leq 10^{-14}$ W/ $\sqrt{\text{Hz}}$ for the regenerative detector of Sec. V.

ACKNOWLEDGEMENTS

The author has profited greatly from discussions with S. A. Sterling, J. Clarke, and R. Y. Chaio during the preparation of this manuscript.

This work was done under the auspices of the U.S. Atomic Energy Commission.

REFERENCES

1. B. D. Josephson, Phys. Letters 1, 251 (1962); Rev. Mod. Phys. 36, 216 (1964); Advan. Phys. 14, 419 (1965).
2. See, for example, C. Kittel, Introduction to Solid State Physics (John Wiley & Sons, Inc., New York, 1966) 3rd ed. pp. 361-363.
3. E. Riedel, Z. Naturforsch. 19a, 1634 (1964).
4. N. R. Werthamer, Phys. Rev. 147, 255 (1966).
5. I. K. Yanson, V. M. Svistunov, and I. M. Dmitrenko, Zh. Eksp. Theor. Fiz. 48, 976 (1965) [Sov. Phys. - JETP 21, 650 (1965)][JETP Lett. 2, 154 (1965)]; I. M. Dmitrenko and I. K. Yanson, Zh. ETF Pis. Red. 2, 242 (1965) [JETP Lett. 2, 154 (1965)].
6. D. N. Langenberg, D. J. Scalapino, B. N. Taylor, and R. E. Eck, Phys. Rev. Letters 15, 294 (1965).
7. S. Shapiro, Phys. Rev. Letters 11, 80 (1963); S. Shapiro, A. R. Janus, and S. Holly, Rev. Mod. Phys. 36, 223 (1964).
8. W. H. Parker, B. N. Taylor, and D. N. Langenberg, Phys. Rev. Letters 18, 287 (1967).
9. J. Clarke, Phil. Mag. 13, 115 (1966); J. Clarke and W. E. Tennant (to be published).
10. P. W. Anderson and A. H. Dayem, Phys. Rev. Letters 13, 195 (1964); A. H. Dayem and J. J. Wiegand, Phys. Rev. 155, 419 (1967).
11. J. Clarke, Phys. Rev. Letters 21, 1566 (1968).
12. C. C. Grimes, P. L. Richards, and S. Shapiro, Phys. Rev. Letters 8, 431 (1966), and J. Appl. Phys. 39, 3905 (1968).
13. N. R. Werthamer, Phys. Rev. 147, 255 (1966); N. R. Werthamer and S. Shapiro, Phys. Rev. 164, 523 (1967).

14. M. D. Fiske, Rev. Mod. Phys. 36, 221 (1964).
15. A. H. Dayem and C. C. Grimes, Appl. Phys. Letters 9, 47 (1966);
J. E. Zimmerman, J. A. Cowen, and A. H. Silver, Appl. Phys. Letters
9, 353 (1966).
16. P. L. Richards and S. A. Sterling, Appl. Phys. Letters 14, 394 (1969);
Phys. Rev. (to be published).
17. C. C. Grimes and S. Shapiro, Phys. Rev. 169, 397 (1968).
18. A. Longacre, Jr. and S. Shapiro, Bull. Am. Phys. Soc. [Ser. II] 14,
856 (1969).
19. H. A. Notarys and J. E. Mercereau, Proceedings of the 1969 Stanford
Conference on the Science of Superconductivity (to be published).
20. D. E. McCumber, J. Appl. Phys. 39, 3113 (1968).
21. T. D. Clark, Phys. Letters 27A, 585 (1968); T. D. Clark and
D. R. Tilley, Phys. Letters 28A, 62 (1968).
22. R. de Bruyn Ouboter and A. Th. A. M. de Wade (to be published in
Progress in Low Temperature Physics Vol. VI, C. J. Gorter, ed.,
(North Holland Pub. Co., Amsterdam).
23. R. C. Jaklevic, J. Lambè, A. H. Silver, and J. E. Mercereau,
Phys. Rev. Letters 12, 159 (1964); 12, 274 (1964); Phys. Rev. 140,
A1628 (1965).
24. J. E. Zimmerman and A. H. Silver, Phys. Rev. 141, 367 (1966);
Phys. Rev. 157, 317 (1967).
25. J. E. Mercereau (to be published).

FIGURE CAPTIONS

- Fig. 1. Riedel Singularity. In the absence of frequency dependent effects in the impedance matching, the spectral response of broadband detector should reflect this singularity.
- Fig. 2. Current-voltage characteristic of a Nb point contact junction coupled to varying amounts of rf power at 24 GHz. The power is zero for the lowest curve. The higher curves were obtained for an increasing power parameter.
- Fig. 3. Two methods of extracting a signal from a step on the junction I-V curve. The (square wave) modulated rf signal causes the I-V curve to jump between the solid and broken curves. (a) The conventional constant current bias method in which a modulated voltage proportional to the differential resistance is obtained. (b) The suggested voltage bias method in which a constant applied voltage bias equal to the step voltage has a small ac modulation. The ac current signal is amplitude modulated by the rf signal.
- Fig. 4. Spectral response of broadband detector from Ref. 12. Response is dominated by resonances in the nominally non-resonant surroundings of the point contacts shown in Fig. 11(D).
- Fig. 5. Spectral response of a broadband detector from Ref. 16. Some of the response peaks are due to identifiable resonances in the co-axial cavity of the type shown in Fig. 11(B).
- Fig. 6. Schematic of regenerative receiver circuit which is analogous to the regenerative Josephson detector. The cavity is represented by a band pass filter with frequency ω_0 and quality factor Q_0 . If the loop gain G_L approaches unity the response is feedback narrowed

so that $Q_R \gg Q_0$.

Fig. 7. Calculated spectral response of the regenerative detector from Ref. 16. The curve for $\Gamma = 0$ is the Lorentzian resonance of the cavity. For larger values of Γ , the feedback narrowing is clearly seen.

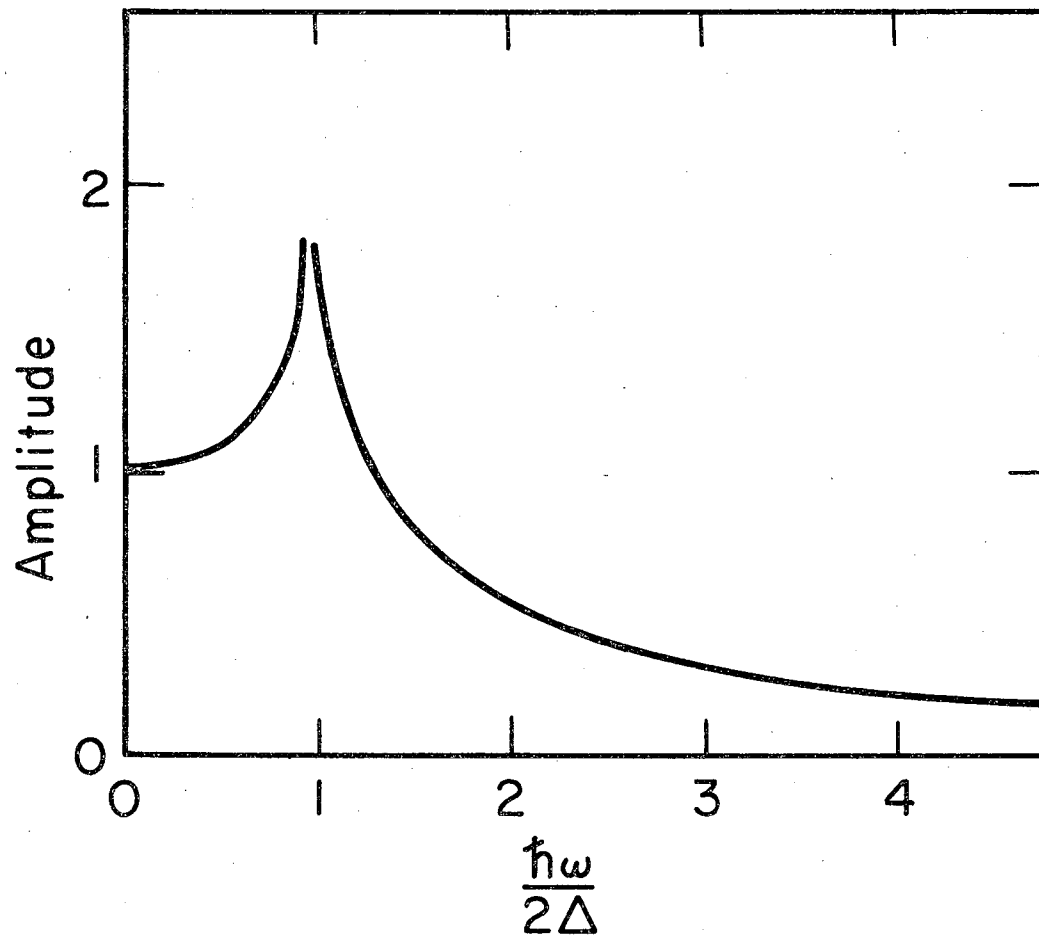
Fig. 8. Characteristics of a junction coupled to a resonant cavity from Ref. 16. The cavity resonance corresponds to $\sim 390 \mu\text{V}$. (a) Direct current, (b) differential resistance (c) response to blackbody radiation.

Fig. 9. Measured spectral response of the regenerative detector from Ref. 16, showing feedback narrowed response peak.

Fig. 10. Current voltage characteristic of a Nb point contact junction coupled to varying amounts of rf power at two closely spaced rf frequencies (64 GHz and 72 GHz) from Ref. 17. Extra steps due to mixing are clearly seen.

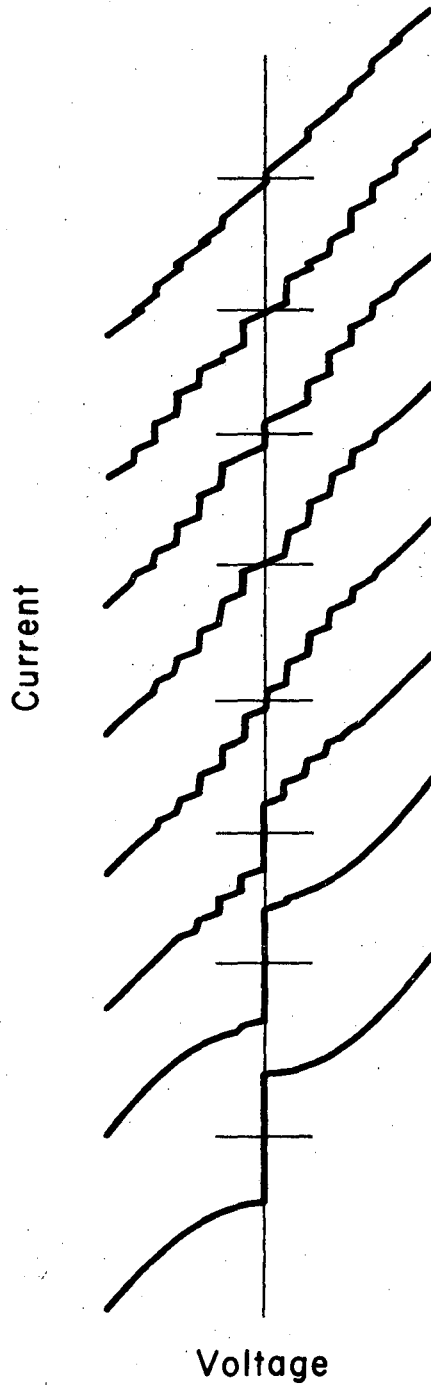
Fig. 11. Various cavities used for coupling infrared radiation to point contacts from Ref. 16.

Fig. 12. Apparatus for holding and adjusting point contacts at He temperature from Ref. 16. The Nb wires S_1 and S_2 are mounted by a screw C through insulating blocks I to a stiff yoke. The yoke is deformed so as to adjust the contact by a differential screw D with nuts N. Radiation reaches the contact via light pipe L and focusing cone F.



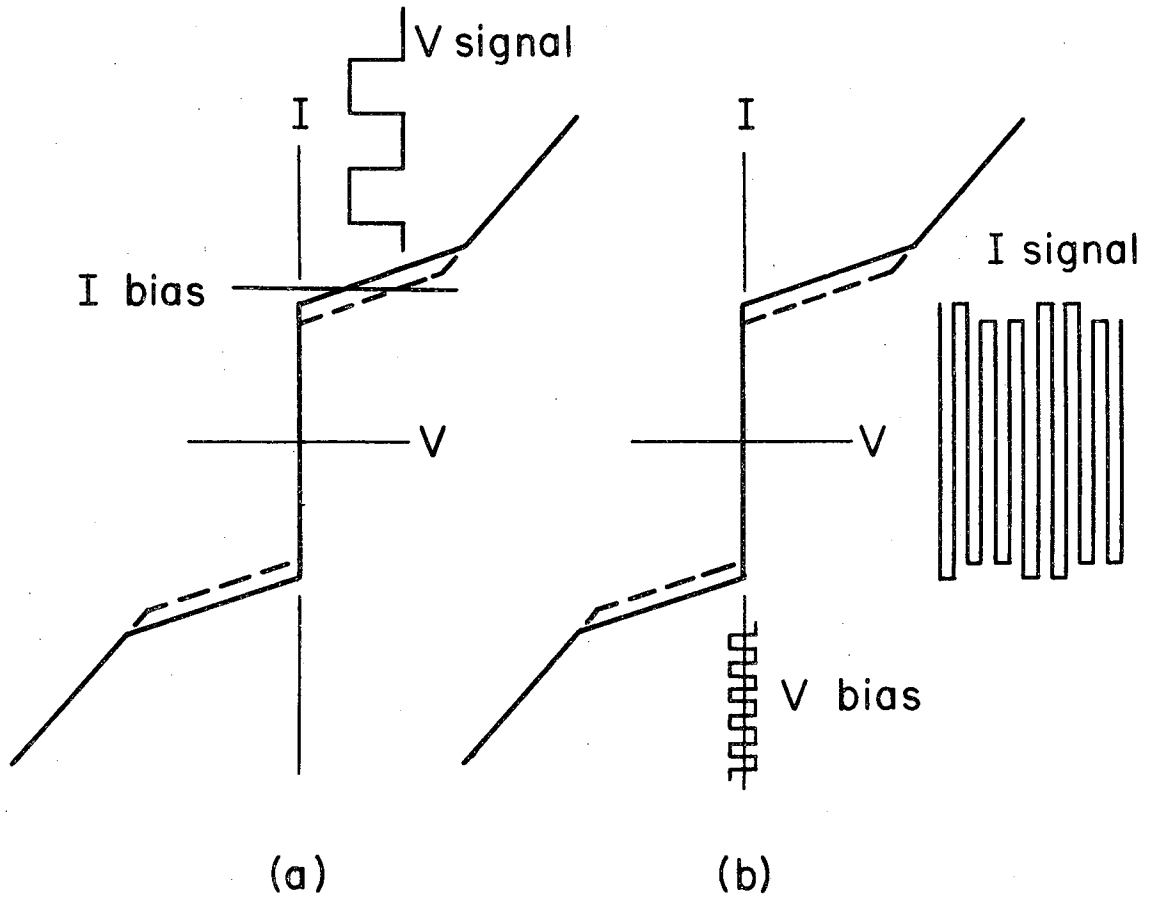
XBL6910-6071

Fig. 1



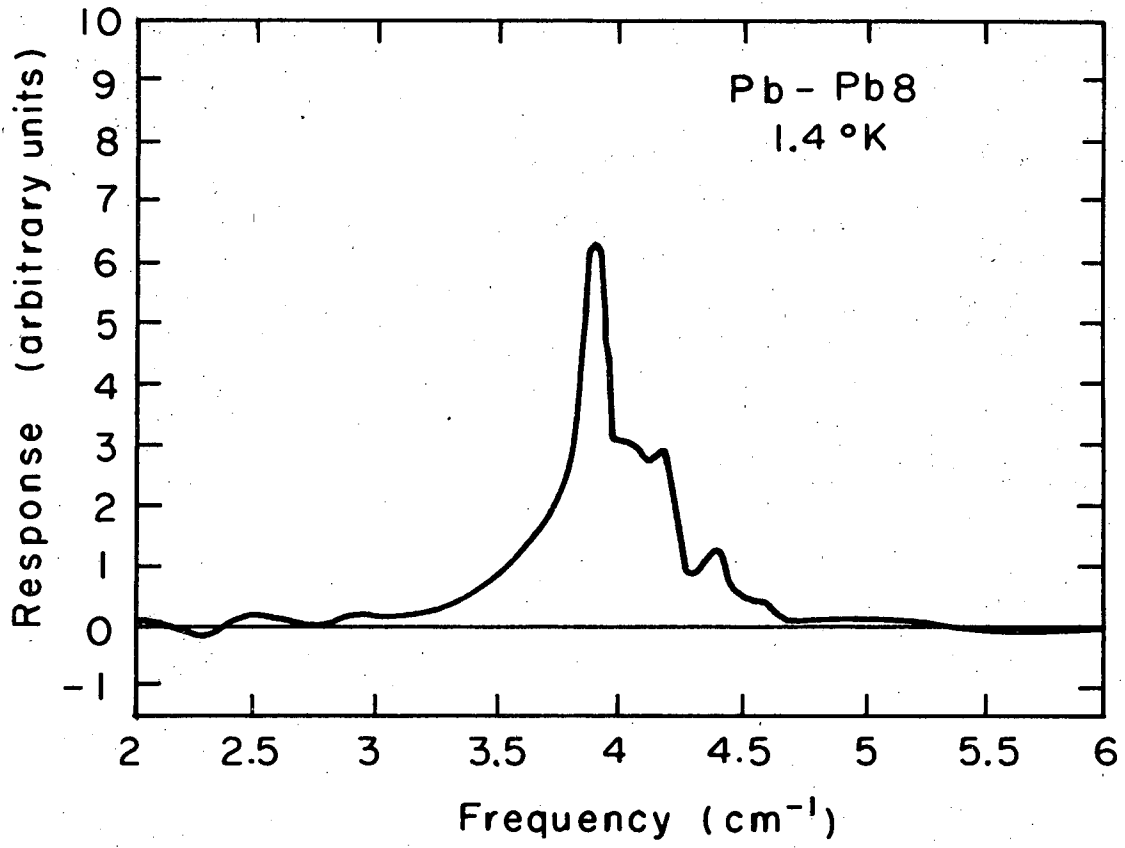
XBL 6712-5855

Fig. 2



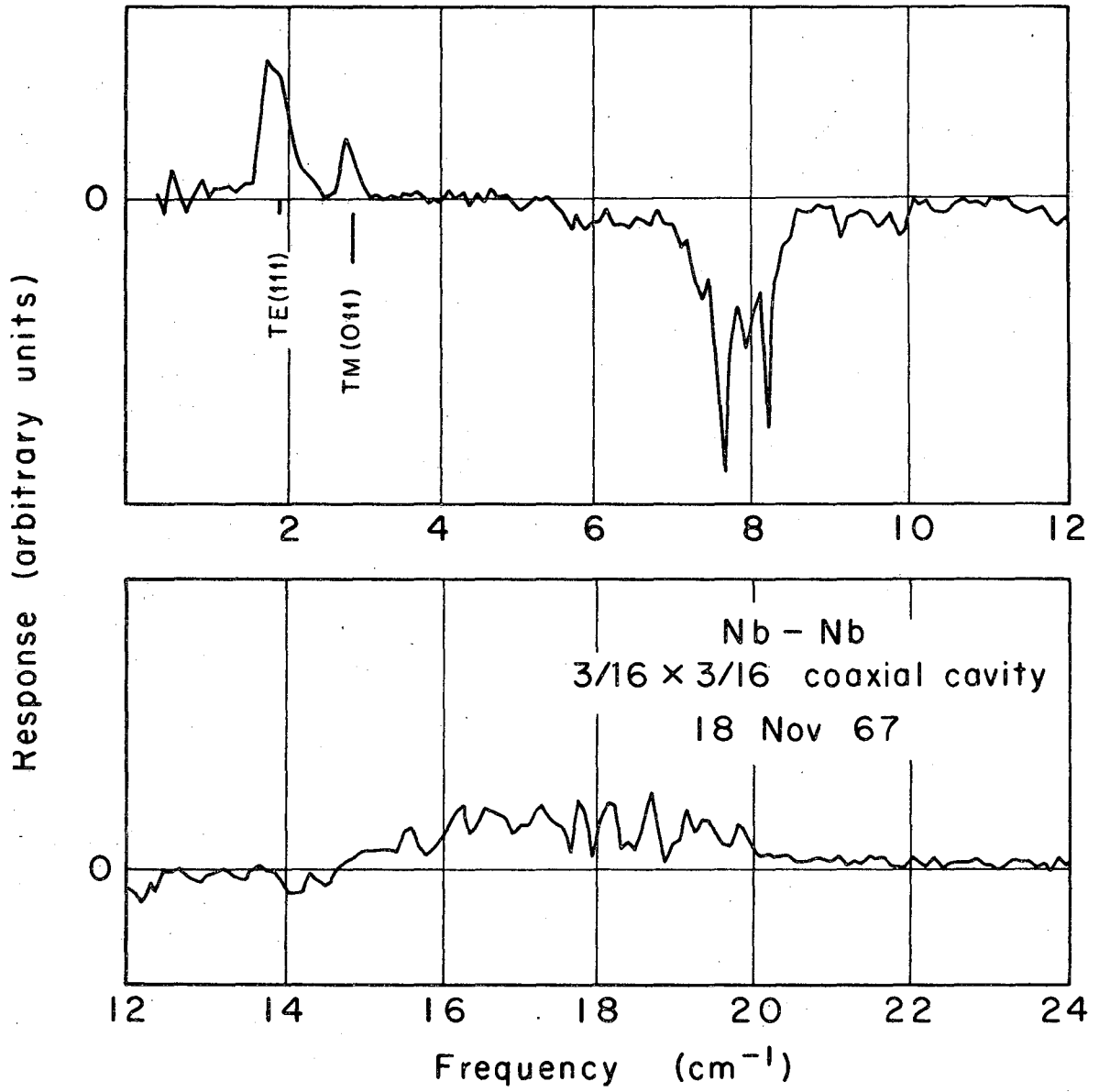
XBL6910-6013

Fig. 3



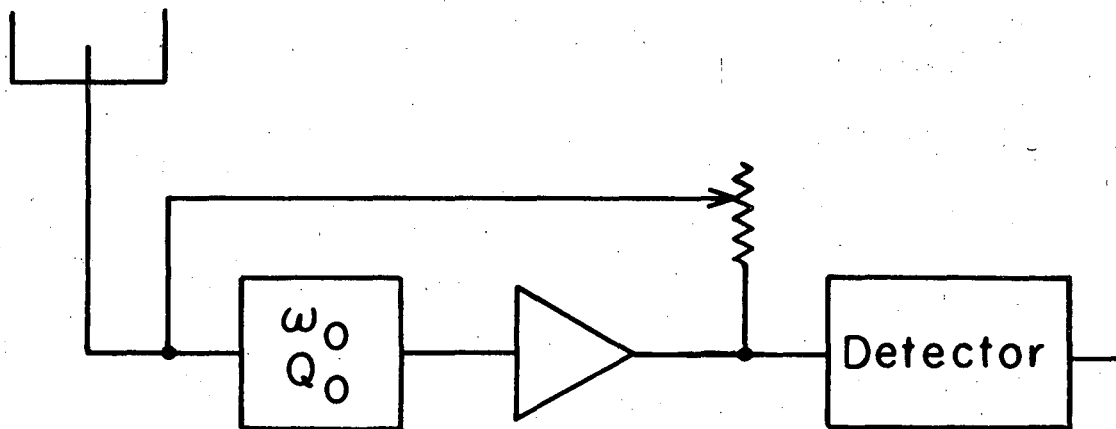
XBL6910-3954

Fig. 4



XBL682-1995

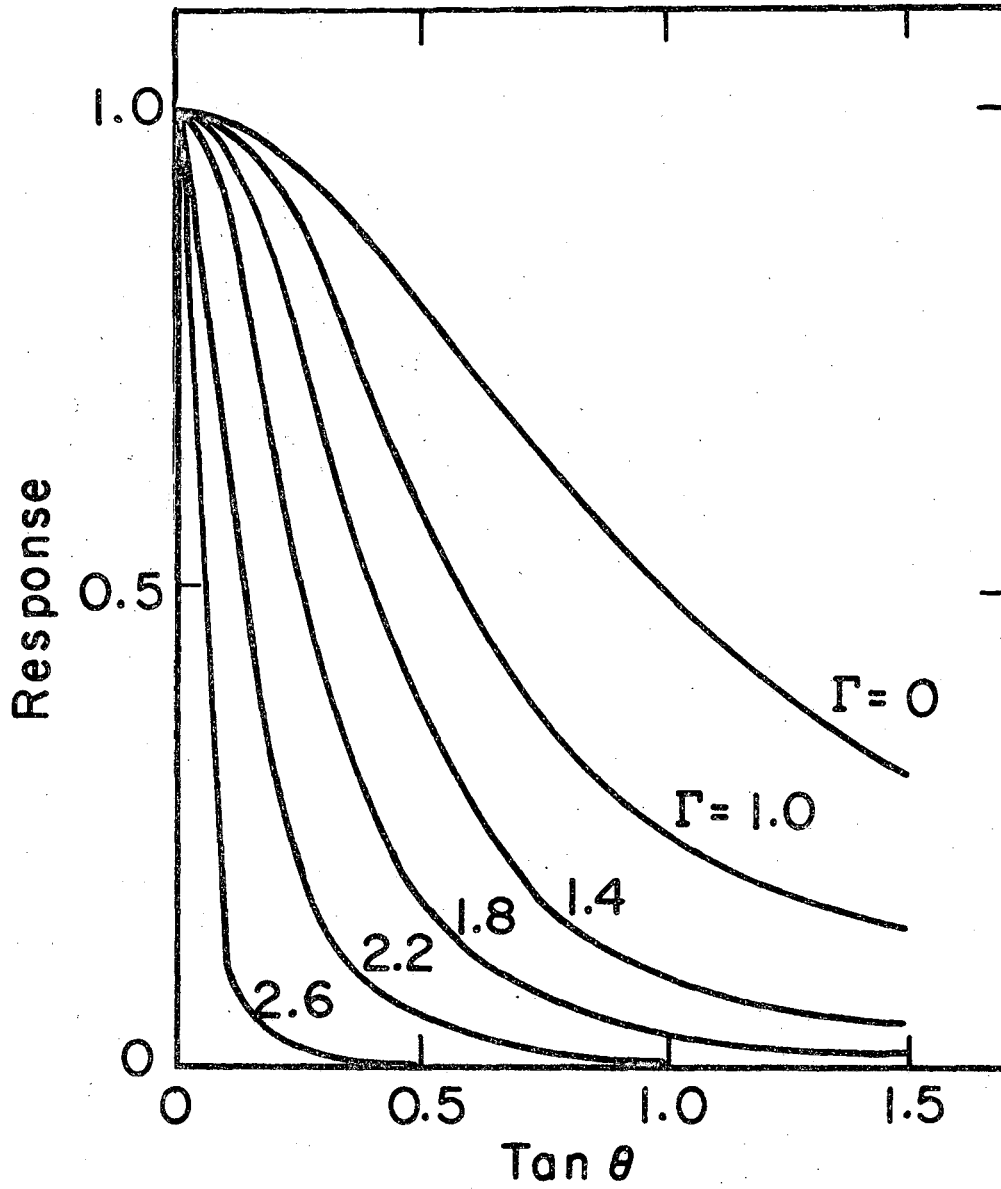
Fig. 5



Response $Q_R \approx Q_0 / (1 - G_L)$

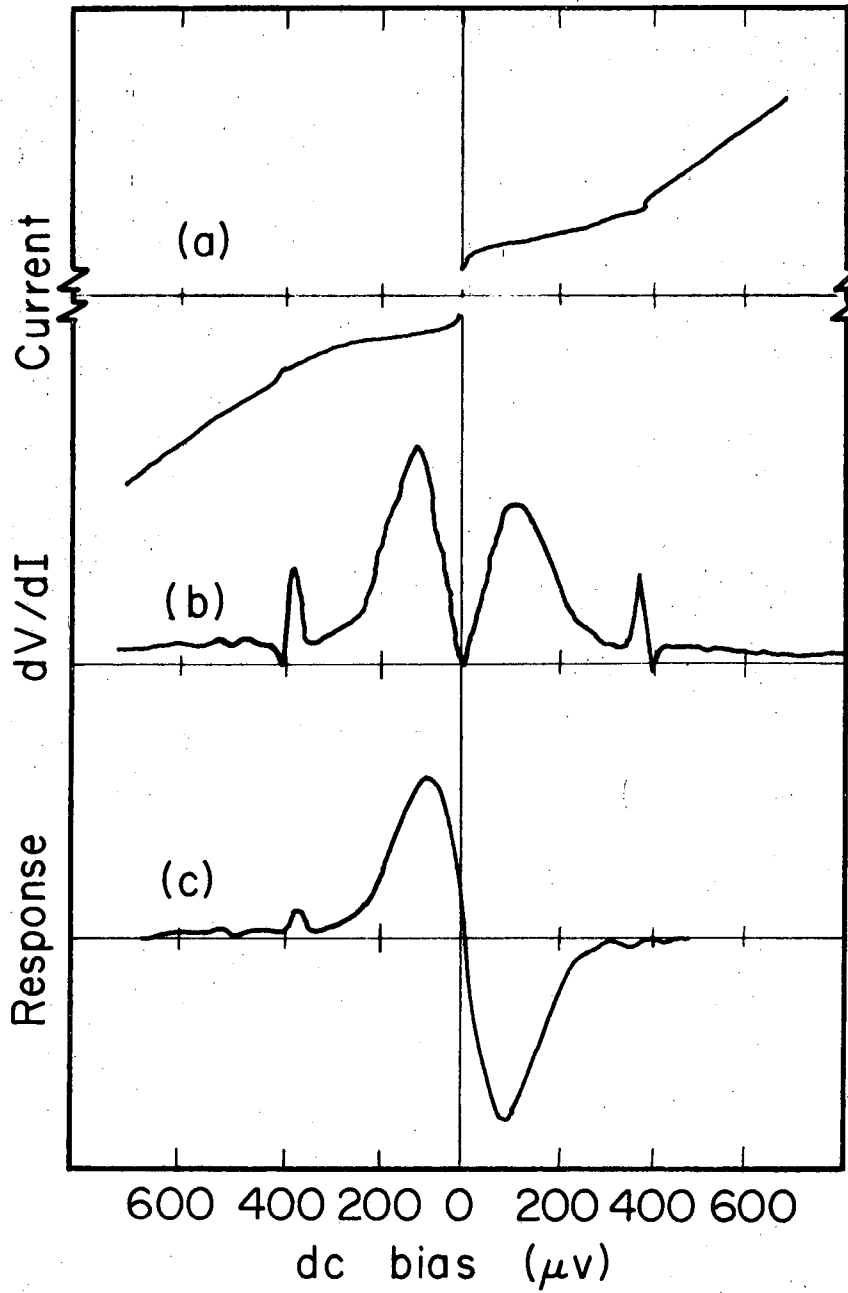
XBL6910-3955

Fig. 6



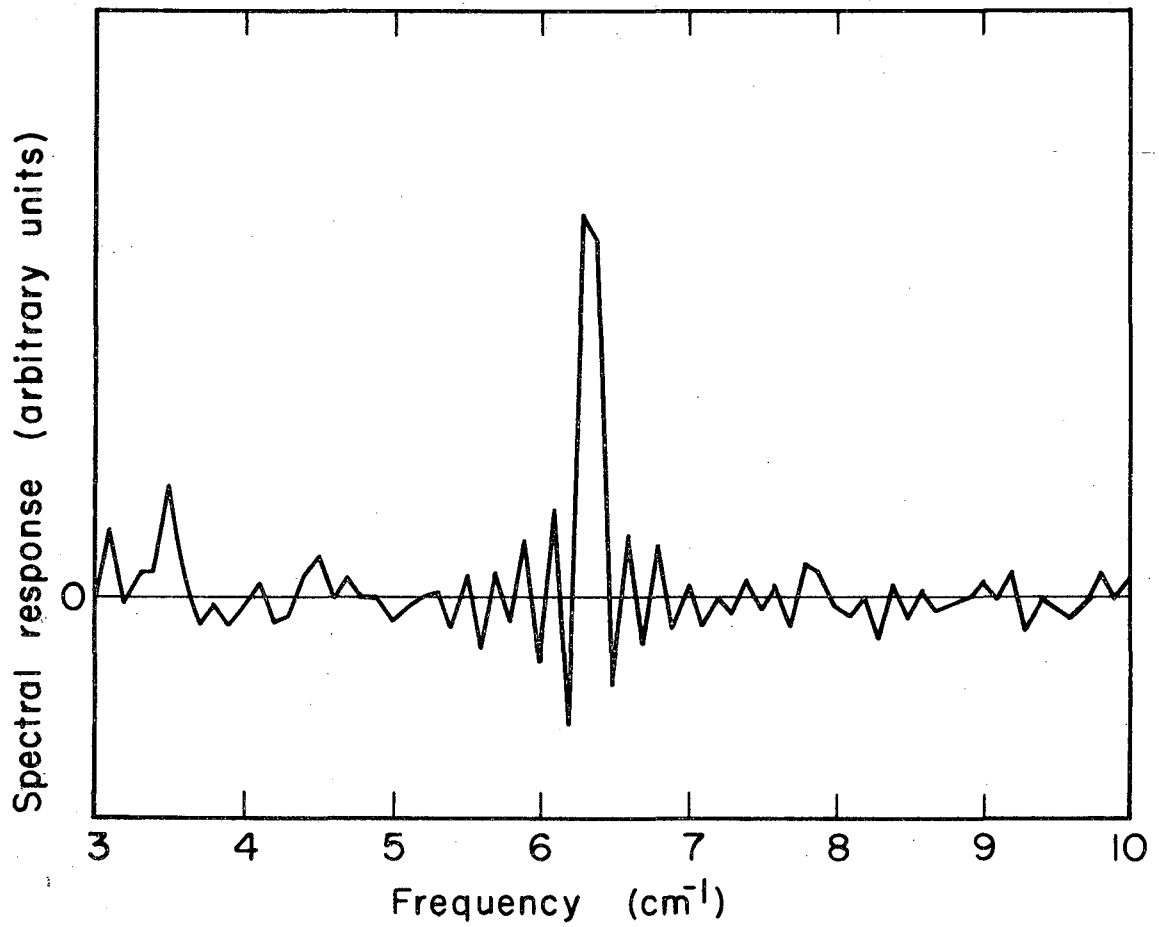
XBL687 - 3199

Fig. 7



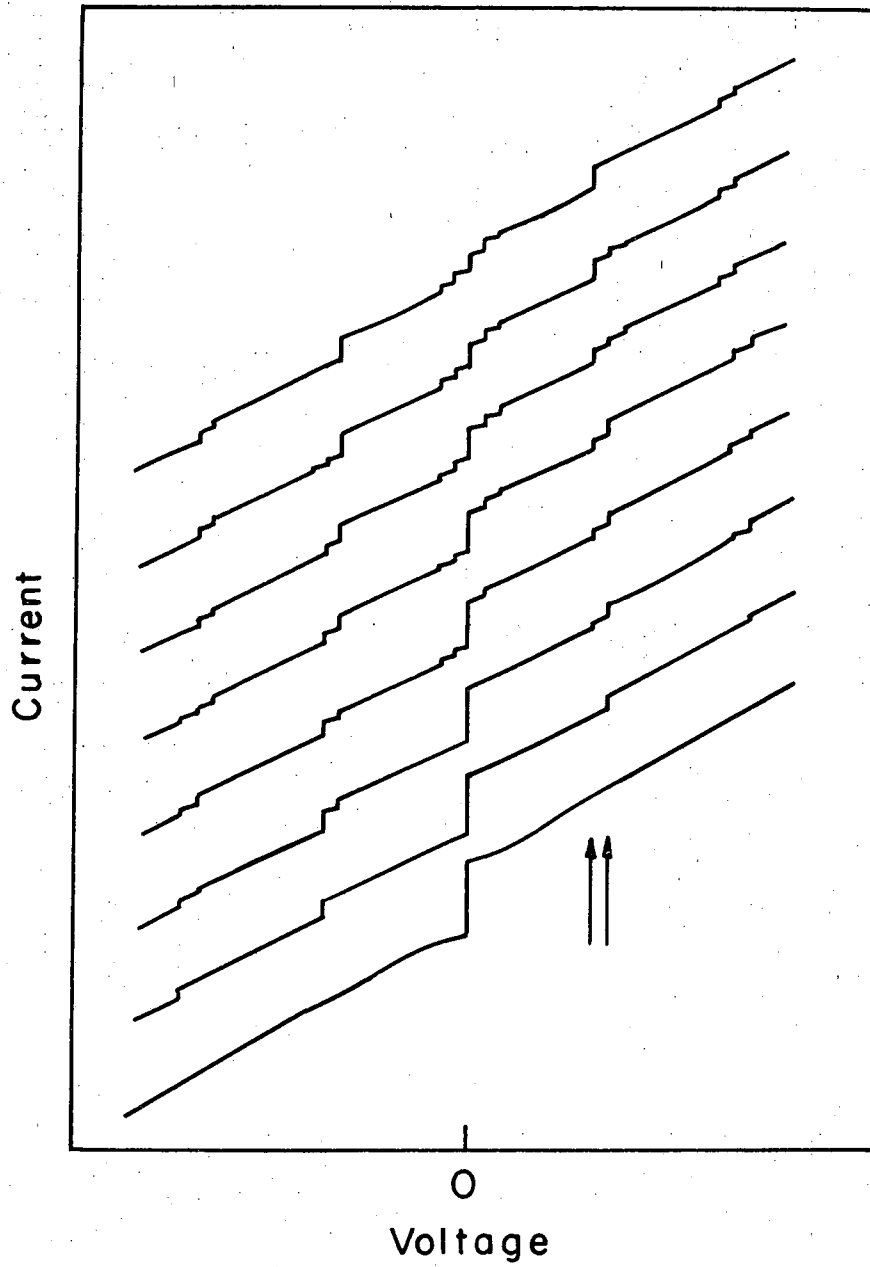
XBL69I-170I

Fig. 8



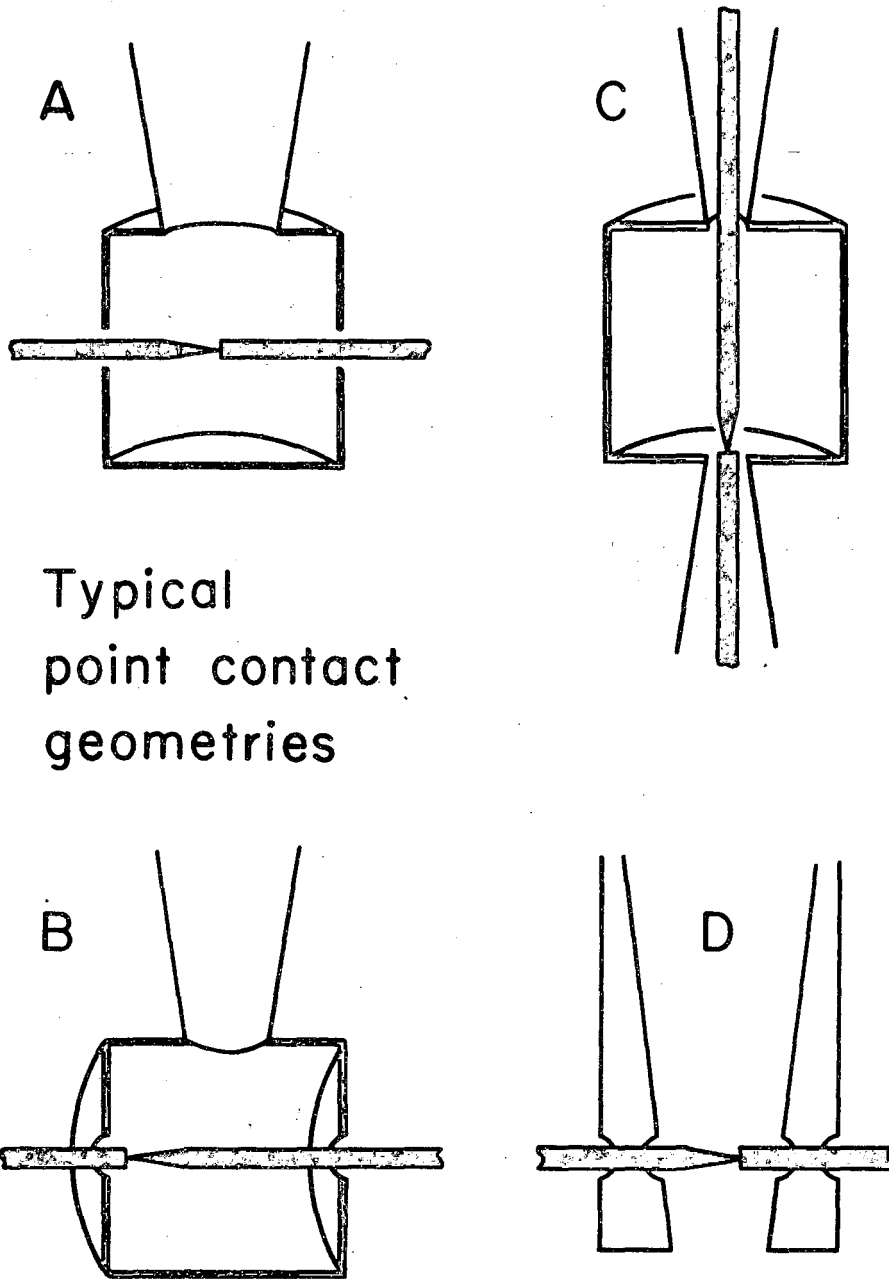
XBL687-3160

Fig. 9



XBL6910-3953

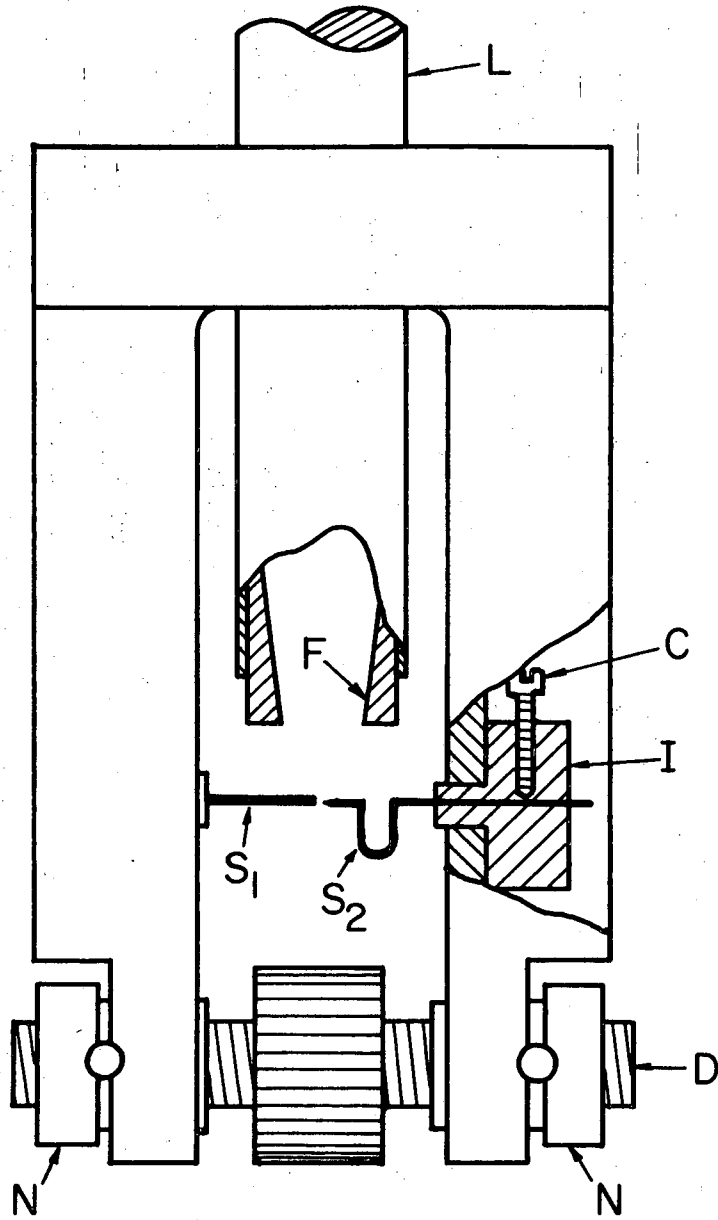
Fig. 10



Typical
point contact
geometries

XBL6910-3934

Fig. 11



XBL 698 - 3401

Fig. 12

LEGAL NOTICE

This report was prepared as an account of Government sponsored work. Neither the United States, nor the Commission, nor any person acting on behalf of the Commission:

- A. Makes any warranty or representation, expressed or implied, with respect to the accuracy, completeness, or usefulness of the information contained in this report, or that the use of any information, apparatus, method, or process disclosed in this report may not infringe privately owned rights; or*
- B. Assumes any liabilities with respect to the use of, or for damages resulting from the use of any information, apparatus, method, or process disclosed in this report.*

As used in the above, "person acting on behalf of the Commission" includes any employee or contractor of the Commission, or employee of such contractor, to the extent that such employee or contractor of the Commission, or employee of such contractor prepares, disseminates, or provides access to, any information pursuant to his employment or contract with the Commission, or his employment with such contractor.

TECHNICAL INFORMATION DIVISION
LAWRENCE RADIATION LABORATORY
UNIVERSITY OF CALIFORNIA
BERKELEY, CALIFORNIA 94720